Electroosmotic Pressure-Driven Flow through a Slit Micro-Channel with Electric and Magnetic Transverse Field

A. Moradmand[1], M. Saghafian[2†] and B. Moghimi Mofrad[3]

Department of Mechanical Engineering, Isfahan University of Technology, Isfahan, Iran

† Corresponding Author Email: saghafian@cc.iut.ac.ir

ABSTRACT

In the present study, flow through two-dimensional microchannel under an axial electric field, transverse electric and magnetic fields and with axial pressure gradient has been investigated numerically. Continuity and momentum equations were solved steadily with respect to the non-slip condition by using discrete finite volume method and a numerical code. The results show that in the presence of the axial electric field, applying transverse magnetic field reduces flow velocity. However, when the transverse electric field and axial electric field exist together, applying the transverse magnetic field increases the flow rate to a certain extent and then reduces the flow rate. Hartmann number like this amount of magnetic field is known as critical Hartmann number. Therefore, with the presence of transverse and axial electric fields and transverse magnetic field, the highest possible flow rate is for critical Hartmann number. It was also found that by increasing the pressure gradient within the microchannel, the critical Hartmann number decreases. Moreover, by increasing the transverse electric field, the sensitivity of critical Hartmann number to the pressure gradient decreases and its value tends to a specific number (about 1.5).

Keywords: Microchannel; Electro-osmotic flow; Electro magneto hydro dynamic; Transverse electrical field; Critical hartmann number.

NOMENCLATURE

b	induced magnetic field	T	absolute temperature
B	applied externally magnetic field strength	u	flow velocity in x-direction
		U	dimensionless flow velocity in x-direction
B_y	applied magnetic field in y-direction	U_{av}	dimensionless average flow velocity
D_h	hydraulic diameter	u_{HS}	Helmholtz-Smoluchowski
e	charge of an electron	u_{av}	average flow velocity in x-direction
E	externally Applied electric field strength	u_{max}	maximum flow velocity in x-direction
E_x	externally Applied electric field in x-direction	U_{max}	dimensionless maximum flow velocity
E_z	externally Applied electric field in z-direction	v	flow velocity in y-direction
		V	flow velocity vector
F	body force vector	w	flow velocity in z-direction
F_{EK}	electrokinetic body force	Y	dimensionless height
H	microchannel half height	Z_i	valency of ith ionic species
H_a	Hartmann number		
Ha_{cr}	critical hartmann number	α	dimensionless electric field in x-direction
J	induced electric current density	ε	relative permittivity of the medium
K_B	boltzmann constant	$ε_0$	permittivity of free space
L	micro channel length	ζ	wall zeta potential
n	ionic number concentration	κ	debye-huckel parameter
n_0	bulk concentration of the ions	K	dimensionless Debye-Huckel parameter
P	pressure	$λ_D$	debye length
R_m	Magnetic Reynolds number	μ	viscosity of the electrolyte
S	dimensionless electric field in z-direction	$ρ_e$	electric charge density
		$ρ_f$	electrolyte density
		σ	electric conductivity of the electrolyte

| φ | electrostatic potential | Ω | dimensionless pressure gradient |
| ψ | electrical double layer potential | | |

1. INTRODUCTION

Due to their numerous advantages and features, micro-electro mechanical systems (MEMS), are used in various fields such as industrial automation, chemical processing, safety and monitoring, medical diagnostics, power and propulsion, and printing and computers (Li, 2008). Fluid transfer mechanism in microchannel is one of the most important issues which should be considered in the evaluation of MEMS systems. Generally, micro-pumps are classified into general categories of mechanical and non-mechanical micropumps (Jang and Lee, 2000). In mechanical micropumps, some moving parts have been used to create the necessary pressure difference for fluid transfer. Due to numerous pressure drops at micro scale and complexity of moving parts fabrication in this scale, fluid transfer in this method may face with serious constraints. Non-mechanical micropumps have no moving parts and external electric and magnetic fields are usually used in them to move the fluid. This method is based on electrokinetic phenomenon which has been developed in a flow and has many applications in medical fields, such as drugs transmission with electrical conductivity characteristics and transfer of test samples. It also has applications in non-medical fields such as pumping a fluid, ionic fluids, mixing fluids, separation of impurities in the materials, flow control, etc (Al-Habahbeh *et al*., 2016). Electrokinetic effect was discovered for the first time by Reuss (1809). He showed that by applying an electrical voltage, water can flow in a conduit made of clay. However, this subject did not attract the attention of researchers for years till finally Smoluchowski provided the first analytical solution for electrokinetic phenomenon in electroosmotic flow in a simple channel and in the presence of Newtonian fluid (Li, 2004). Burgreen and Nakache (1964) examined electrokinetic flow of a Newtonian fluid in a microchannel consists of two parallel plates. After them, Rice and Whitehead (1965) used Debye-Huckel approximation for low zeta potential to investigate extended electro-osmotic flow in a circular cross section. Levine *et al*. (1975) studied electrokinetic flow in cylindrical channels at high zeta potential (approximately 100-200 mV) to develop the method of Rice and Whitehead (1965).

Yang and Li (1997) examined electro-osmotic flow under a pressure gradient in a rectangular microchannel. To do so, non-linear Poisson-Boltzmann equation was once solved numerically using finite-difference method and once analytically using Green's function method. They stated that induced electrokinetic potential increases as the pressure difference increases, however, it decreases with an increase in the ionic concentration in solution. Patankar and Hu (1998) also provided a numerical solution for electro-osmotic flow in complicated geometries using computational fluid dynamics. Arulanandam and Li (2000) analyzed and examined an electro-osmotic flow of a Newtonian fluid in a rectangular microchannel. They solved Poisson-Boltzmann and momentum equation by the finite-difference method in two dimensions and obtained velocity distribution within the microchannels in terms of flow parameters. In this research, the effect of various factors such as the cross-sectional geometry, channel dimensions, zeta potential, ion density and the electric field on the velocity field and volumetric flow rate has been examined. Wang *et al*. (2004) conducted a work for simulation of two-dimensional fully developed laminar flow. They added Lorentz force to momentum equation as a source term instead of using the analytical solution of the Lorentz force applied to the fluid caused by magnetic field in momentum equation. The obtained velocity profile from this method is in good agreement with the experimental results.

Chakraborty and Paul (2006) examined fluid flow under the effect of controlling forces of electromagnetohydrodynamic (EMHD) inside the microchannels which consists of two parallel plates by considering the pressure gradient. For a specific applied pressure gradient, the effect of electric and magnetic fields were analyzed. They showed that by using a relatively low-strength magnetic field and in the presence of a transverse electric, the volumetric flow rate increases. However, for a very high-strength magnetic field and in the presence of a transverse electric field, volumetric flow rate decreases. Deng *et al*. (2012) studied unsteady electro-osmotic flow of a non-Newtonian fluid in a rectangular microchannel. They used linear Poisson-Boltzmann equation obtained distribution of electric potential and solved the obtained momentum equations by using finite-difference method. In addition, the effects of fluid properties and geometric characteristics of the channel have been studied and then they expressed that by increasing the Debye-Huckel parameter, velocity distributions in the channel tend to become more uniform. Chakraborty *et al.* (2013) were the first researchers who studied heat transfer characteristics of thermally fully developed electromagnetohydrodynamic flow between two parallel plates, under constant wall heat flux. They studied the effects of magnetic and electric fields on heat transfer by taking into account the viscous dissipation and Joule heating. Their results indicate that for a specific value of applied pressure gradient and the axial electric field, heat transfer characteristics in micro-scales can significantly change by controlling the applied magnetic field and transverse electric field.

Escandón *et al*. (2014) conducted an analytical study on the flow field and the temperature of a viscoelastic fluid in a rectangular microchannel under the simultaneous effect of electric and magnetic fields

and pressure gradient. Their results showed that in the presence of electric and magnetic fields compared to the time when only the electric field is applied, without any increase in maximum temperature of the fluid, the volumetric flow rate increases approximately 40%. Moreover, the volumetric flow rate of Newtonian fluid flow compared to viscoelastic fluids is more sensitive to magneto hydrodynamic forces. Kiyasatfar and Pourmahmoud (2016) dealt with the numerical analysis of heat transfer and fully-developed steady laminar flow of an electrically conducting non-newtonian fluid in a square microchannel, under a transverse magnetic field and taking into account the effects of viscous dissipation and Joule heating. The governing equations have been solved using finite difference method under the assumption of no slip condition and constant wall flux. The results indicated that an increase in Hartmann number reduces the maximum velocity of the fluid in the channel and increases the near-wall velocity gradient and results in a more uniform velocity profile. Moreover, Nusselt number reduces by an increase in the amount of viscous dissipation and Joule heating. In addition, the effect of Hartmann number on temperature field and Nusselt number depend on Brinkman number, and the severity of this dependence is defined as a function of the flow behavior index. Wang *et al.* (2016) conducted a study using Perturbation techniques and numerical solutions for EMHD flow of non-Newtonian fluids between two parallel micro-plates. They have found that in a particular fluid and electrical field, an increase in Hartmann number significantly reduces convection and thus reduces the temperature and velocity. However, the increase in the electric field strength increases the velocity distribution and temperature in a specific Hartman.

The present study examines magneto electrohydrodynamic flow behavior of a Newtonian fluid in a two-dimensional microchannel in the presence of pressure gradient. For this purpose, flow equations under external fields are numerically solved at steady state by using finite volume method. Then, the effects of electric and transverse and axial magnetic fields on fluid flow inside the microchannels are investigated. Finally, in each transverse electric field, the critical Hartmann number was presented based on fluid flow in the microchannel.

2. MATHEMATICAL MODELING

2.1 Problem Definition and Assumptions

In this article, the fluid flow through a microchannel between two parallel plates is studied under the constant and uniform electric and magnetic field. According to Fig. 1, a microchannel with height 2H, length L and under an axial electric field E_z along the x-axis has been presented. In addition, two transverse electric and magnetic fields perpendicular to the microchannel axis are applied: a transverse magnetic field B_y along a y-axis and a transverse electric field E_z in opposite direction of the z-axis. Coordinate axis

is set in such a way that the x-axis is along the axis of channel microchannel and in line with it, there is an axial pressure gradient.

Fluid examined in this study is a symmetric electrolyte solution ($z_+ = z_- = z$) which is Newtonian and incompressible and has constant physical properties. Moreover, according to aspects of the problem and physical properties of the fluid, the manetic Reynolds number $R_m = \mu\sigma uH$ <<1.0 has been assumed. The electrolyte solution is normally neutral. However, if it is in contact with the charged surface, electric double layer (EDL) is created near the surface. Nonhomonymous ions of the surface are attracted to the wall and form the Stern layer. Then, immediately stern layer forms diffuse layer where the ion density variation obeys the Boltzmann distribution (Li, 2004). The thickness of the layer depends on the concentration of the electrolyte solution and its electrical properties. The plane between the stern and diffuse layers in EDL is called the shear plane. Ions distribution through the EDL is shown by electric potential parameter ψ. Electric potential on the surface of the wall is called wall potential ψ0 and the electrical potential caused by the ions arrangement on the shear plane is called zeta potential ζ (Nguyen and Wereley, 2002). Finally, the movement of ionized liquid relative to the stationary charged surface which is as a result of an external electric field is called electro-osmotic flow (Karniadakis *et al.* 2006).
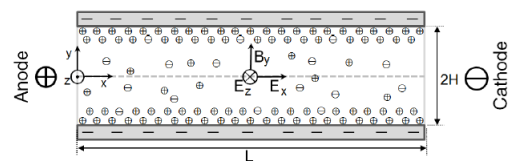

Fig. 1. Channel view under external applied electric field

2.2 Governing Equations

in an incompressible and steady fluid flow with constant properties, the continuum and momentum equations under electric and magnetic fields are expressed as follows:

$$\nabla . \vec{V} = 0 \tag{1}$$

$$\rho_f (\vec{V} (\vec{V} . \nabla)) = -\nabla P + \mu \nabla^2 \vec{V} + \vec{F} \tag{2}$$

where $\vec{V} = u\hat{i} + v\hat{j} + w\hat{k}$ indicates the velocity field, ρ_f fluid density, P pressure, μ the fluid viscosity, $\vec{F}$ volumetric force resulting from the application of electric and magnetic fields which can be obtained from the following equation (Chakraborty and Paul, 2006):

$$\vec{F} = \vec{F}_{EK} + \vec{J} \times \vec{B} \tag{3}$$

where $\vec{B}$ is the overall magnetic field applied to the

channel which is expressed as $\vec{B} = B_y \hat{j} + \vec{b}$ .In this equation, $B_y \hat{j}$ is magnetic field applied to the channel in the direction of the axis y and $\vec{b}$ is induced magnetic field caused by charged particle motions inside the channel. However, for small values of the magnetic Reynolds number ($R_m \ll 1.0$), induced magnetic field is insignificant compared to the external magnetic field and the effect of fluid flow on the magnetic field is negligible $\vec{B} = B_y \hat{j}$ (Davidson, 2001). $\vec{J}$ is induced electric current density and $\vec{F}_{EK}$ Electrokinetic volumetric force, or the force resulting from the application of electric fields on the fluid (electroosmotic force) and are obtained from equations 4 and 5, respectively (Davidson, 2001, Masliyah and Bhattacharjee, 2006).

$$\vec{J} = \sigma(\vec{E} + \vec{V} \times \vec{B}) \tag{4}$$

$$\vec{F}_{EK} = \rho_e \vec{E} \tag{5}$$

where σ is electrical conductivity of the fluid, $\vec{E} = E_x \hat{i} + E_z \hat{k}$ external electric field and is obtained using the equation $\vec{E} = -\nabla_\Phi$, where electric potential φ is caused by the voltage applied to the electrodes(Karniadakis *et al.* 2006). The Eq.5 is for the case where there is a homogeneous and singlephase liquid (Karniadakis *et al.* 2006). In this equation, σe is electric charge density caused by the accumulation of oppositely charged ions near the wall (Masliyah and Bhattacharjee 2006).

$$\rho_e = \sum_i z_i e n_i \tag{6}$$

where z is absolute value of the ionic valence in the electrolyte, e the electron charge, and n the ionic number concentration. Moreover, n_i is the ionic number concentration of the ion i located in a specific location can be expressed as a function of the electric potential of the same location and is calculated by Boltzmann distribution equation $n_i = n_0 \exp(-\frac{z_i e \psi}{k_B T})$ (Masliyah and Bhattacharjee, 2006). In this equation, n_i is the number concentration of ion i, n0 ionic concentration of ion i in neutral condition, z_i valence number of ion i, k_B Boltzmanns constant and T temperature and ψ electric potential caused by the electric double layer. By combining the Eq. 6 and Boltzmann distribution and with the assumption of symmetric electrolyte ($z_+ = z_- = z$), Eq. 6 is changed into the following equation.

$$\rho_e = -2zen_0 \sinh(\frac{ze\psi}{k_B T}) \tag{7}$$

To obtain the electric potential distribution and concentration of ions caused by the presence of a charged surface in a neutral dielectric environment is created, Poissons equation can be used as follows, (Masliyah and Bhattacharjee, 2006):

$$\nabla^2 \psi = -\frac{\rho_e}{\varepsilon \varepsilon_0} \tag{8}$$

where ε0 is the vacuum permittivity (electric field distribution due to the concentration of ions in a vacuum), and ε is the dielectric constant of the electrolyte solution. By substituting Eq. 7 in Eq. 8, Poisson-Boltzmann equation governing the electric potential distribution caused by the electric double layer can be obtained. For a microchannel consists of two parallel planes, one-dimensional Poisson-Boltzmann equation is used.

$$\frac{d^2 \Psi}{dy^2} = \frac{2zen_0}{\varepsilon \varepsilon_0} \sinh(\frac{ze\psi}{k_B T}) \tag{9}$$

By defining the non-dimensional electric potential Ψ = zeψ/(k_BT), if the electric potential is small compared to the thermal energy of the ions, i.e. |zeψ| < |kBT | → Ψ ≪ 1 , in Eq. 9 an approximation sinh (Ψ) = Ψ with sufficient accuracy can be done. This approximation is called the linear Debye-Huckel approximation (Li, 2004). For a better understanding, in a solution with a temperature of 25 °C ,if the potential of the surface is ψ ≪ 25.7mV , then Ψ ≪ 1 (Hunter, 2013). With defining Debye-Huckel parameter $\kappa = (\frac{2n_0 z^2 e^2}{\varepsilon \varepsilon_0 k_b T})^{\frac{1}{2}}$ the simplified Poisson-Boltzmann equation which represents the electric potential distribution ψ in the electric double area can be obtained.

$$\frac{d^2 \psi}{dy^2} = \kappa^2 \psi \tag{10}$$

By means of Eq.10, ψ is calculated, and then by using the Eq. 8 , ρ_e can be obtained. By adding the results in Eq. 5, the value of F_{EK} can be achieved. Finally simplified momentum equation for the electro-osmotic flow in a two-dimensional microchannel under applied magnetic and electric fields can be obtained as follows: Momentum in the direction of x:

$$\rho_f \left[u \frac{\partial u}{\partial x} + v \frac{\partial u}{\partial y} \right] = -\frac{\partial P}{\partial x} + \mu \left[\frac{\partial^2 u}{\partial x^2} + \frac{\partial^2 u}{\partial y^2} \right]$$
$$+ \rho_e E_x - \sigma E_z B_y - \sigma u B_y^2 \tag{11}$$

Momentum in the direction of y:

$$\rho_f \left[u \frac{\partial v}{\partial x} + v \frac{\partial v}{\partial y} \right] = -\frac{\partial P}{\partial y} + \mu \left[\frac{\partial^2 v}{\partial x^2} + \frac{\partial^2 v}{\partial y^2} \right] \tag{12}$$

In this article dimensions, velocity, transverse and axial electric field, magnetic field, and pressure gradient are expressed non-dimensionally.

$$Y = \frac{y}{H} \qquad u_{HS} = -\frac{\xi\varepsilon\varepsilon_0 E_x}{\mu} \qquad U = \frac{u}{u_{HS}}$$

$$U_{max} = \frac{u_{max}}{u_{HS}} \quad U_{avg} = \frac{u_{avg}}{u_{HS}} \qquad Ha = HB\sqrt{\frac{\sigma}{\mu}}$$

$$\alpha = \frac{E_x L}{\xi} \qquad S = \frac{HE_z}{u_{HS}}\sqrt{\frac{\sigma}{\mu}} \qquad \Omega = \frac{H^2}{\mu u_{HS}}\frac{dP}{dx}$$

$$\Psi = \frac{ze\psi}{k_B T} \qquad K = \kappa H \qquad R_m = \mu\sigma uH \quad (13)$$

2.3 Boundary Conditions

The governing equations are solved by taking into account the following boundary conditions.

Inlet:

$$u = u_{in}, \qquad v = 0, \qquad \psi = 0 \qquad (14)$$

where u_{in} is velocity in the input cross-section Outlet:

$$\frac{\partial u}{\partial x} = 0, \qquad \frac{\partial v}{\partial x} = 0, \qquad \psi = 0 \qquad (15)$$

Wall condition:

No slip: $u = 0$ at $y = \pm H$ (16a)

$\psi = \zeta$ at $y = \pm H$ (16b)

2.4 Numerical Procedure

The obtained equations are discretized by using a numerical code as finite-volume with the implementation of QUICK method on a collocated grid, and they have been resolved by applying SIMPLEC pressure-correction algorithm. In order to evaluate independence of the solution from the grid, simple flow through a two-dimensional microchannel (between two parallel plates) without a magnetic field and without transverse and axial electric fields has been resolved for grids with nodes 50×10, 100×20, 200×40 and 400×80.

In Fig. 2 developed velocity profile in a microchannel cross-section for four grids has been considered. Since with a change in the solution grid, from grid 200×40 to grid 400×80, the percentage of change is very low (approximately 0.28%), the grid 200×40 is selected to solve the problem.

2.5 Results Validation

In this section, by using the obtained grids in the previous section (grid 200×40), the results of this study are validated. To validate the results obtained from combining electric fields and magnetic field for fluid flow through a long, narrow parallel-plate channel with a gap height of about 200 μm, Chakraborty *et al.* (2013) results have been used. To validate the obtained results from applying a single magnetic field on fluid flow through a parallel plate channel, Lahjomri *et al.* (2003) results have been used. Fig. 3a shows the transverse changes in

developed velocity of flow in a microchannel influenced by axial and transverse electric field and transverse magnetic field. Non-dimensional magnetic field (in the direction of the axis y) with Ha=0.5, non-dimensional transverse electric field (in the direction of the axis z) with S=50, and non-dimensional axial electric field (in the direction of the axis x) with α = 4500 are applied to the fluid flow. In addition, non-dimensional Debye-Huckel parameter is K = 4, and non-dimensional pressure difference is Ω = 1. As can be seen, the profile obtained in this study almost conforms to the velocity profile provided by Chakraborty *et al.* (2013). Fig. 3b shows developed velocity profile within a microchannel flow under the influence of transverse a magnetic field in the direction of the axis y with Ha=5 and non-dimensional pressure Ω = 1. As can be seen, the answer derived from this study fully conforms to the Lahjomri *et al.* (2003) developed velocity profile.
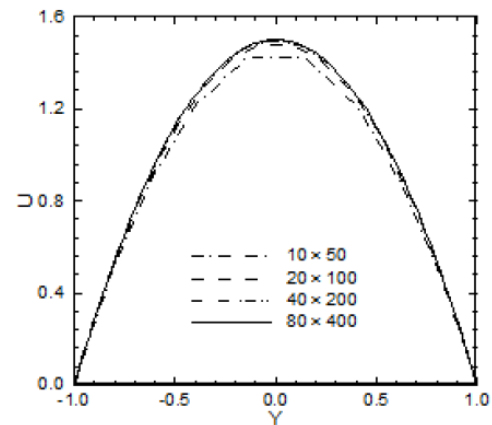
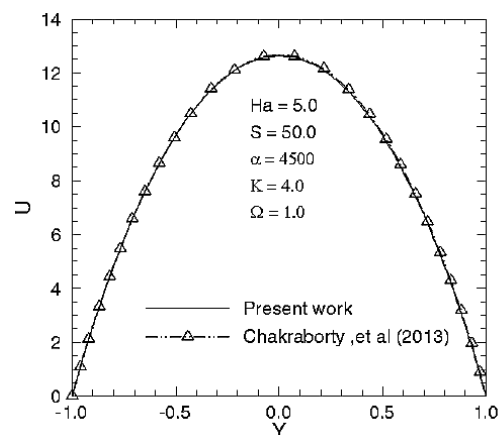**Fig. 2. Examining the independency of the solution grid, non-dimensional velocity diagram.**

Fig. 3. Developed velocity diagram in microchannel cross-section under the influence of (a) Ha=0.5, S=50, α = 4500, K=4, Ω = 1. (b) Ha=5 and Ω = 1.

3. RESULTS

Fig.4 shows graph of developed flow velocity within the microchannel under the influence of various axial electric field and transverse magnetic

field and transverse electric field regardless of the transverse electric field. In this case, the non-dimensional axial electric field (along the axis x) with the value of $\alpha = 4500$, the magnetic field perpendicular to the axis of the microchannel (in the direction of the axis y) with different values of Hartmann numbers in constant non-dimensional axial pressure difference $\Omega = 1$, and K = 1 have been applied to the fluid. Since in this figure axial pressure difference within the microchannel has been considered constant, changing the axial force applied to the fluid changes the flow rate. As can be seen in Figure, as Hartmann number increases, flow velocity (and therefore flow rate) decreases. The existence of axial electric field creates electrokinetic force to the fluid. The term $\rho_e E_x$ on the right hand side of the momentum equation (Eq. 11) represents the axial force. Electric density of the electrolyte solution (ρ_e) near the wall has the maximum value and is negligible in other areas. The electrokinetic force is applied into the near-wall fluid and makes it move. Due to molecular diffusion of momentum, momentum applied to the near-wall fluid is transferred to fluid layers away from the wall. The velocity profile in the channel under the influence of axial pressure gradient is parabolic. However, in the absence of pressure gradient under the influence of electrokinetic force, electro-osmotic flow with flatter velocity profile is created. If a transverse magnetic field (B_y) is applied to the fluid flow within the microchannel which is under the influence of pressure difference and axial electric field, as mentioned in the governing equations, a force which is against the direction of flow $-\sigma u B_y^2$ is applied to the fluid. With the increase in transverse magnetic field (increasing Hartmann number Ha), more deterrent force applied to the fluid which reduces the velocity in the microchannel. However, the existence of axial electric field makes the electro-osmotic force apply to the fluid surrounding the wall. This may make the velocity near the wall of channel become greater than the flow rate in the axis of the channel; moreover, the concavity of profile velocity may change in microchannel cross-section. As can be seen in Fig. 4 this phenomenon occurs at high Hartmann numbers.
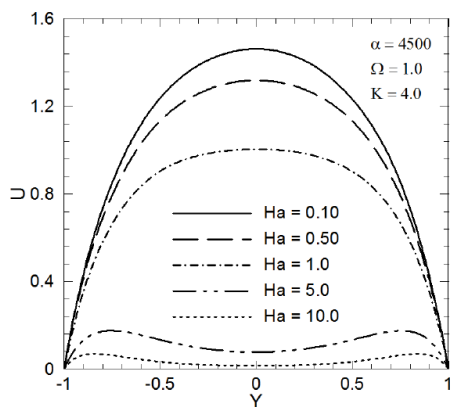

Fig. 4. Developed velocity diagram in microchannel cross-section under the influence of a transverse magnetic field and $\alpha = 4500$.
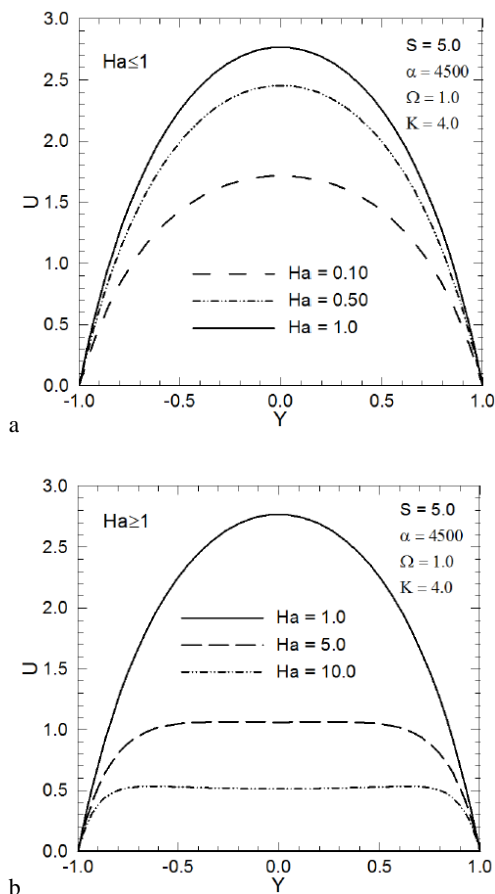

a

b

Fig. 5. Developed non-dimensional velocity diagram in microchannel cross-section under the influence of S=5, $\alpha = 4500$, K=4, $\Omega = 1$ for a. Ha ≤ 1, b. Ha ≥ 1.

Fig. 5a shows the influence of applying a non-dimensional axial electric field $\alpha = 4500$ and the non-dimensional transverse electric field S=5 on velocity profile of flow in a microchannel for Ha ≤ 1 , K=4 and non-dimensional pressure difference Ω. As can be observed, in this range of Hartmann number, the existence of transverse electric field has led to a situation in which the velocity changes are opposite the time no-transverse electric field is present. This means that in this case, as Hartmann number increases, flow velocity increases. Fig. 5b shows the influence of applying a non-dimensional axial electric field $\alpha = 4500$ and the non-dimensional transverse electric field S=5 on velocity profile of flow in a microchannel in numbers Ha ≥ 1, for K=4 and non-dimensional pressure difference$\Omega = 1$. As can be seen, velocity changes for this range of Hartmann number despite the presence of transverse electric field are opposite the Ha ≤ 1 numbers (Fig.5a). In the range of Ha ≥ 1, as Hartmann number increases, flow velocity decreases like the time the transverse electric field is not present. This phenomenon has also been reported by Chakraborty *et al.* (2013). According to Fig. 5, apparently when the transverse electric field is present, with an increase in Hartmann number to a certain amount, flow velocity increases and after that the flow velocity decreases by increasing Hartmann number. This specific amount of Hartmann number is called

critical Hartmann number (Ha$_{cr}$) (Chakraborty *et al.* (2013)). In Fig. 6a maximum velocity diagram has been plotted for S=0.5 and in Fig. 6b the maximum velocity has been plotter for S=5, according to Hartmann number. These figures are plotted for α = 4500, K = 4, and the non-dimentional pressure difference Ω = 1. By using Fig. 6 the exact amount of critical Hartmann number for transverse electric fields S=0.5 and S=5 can be achieved. This value for S=0.5 equals 0.188 and for S=5 equal to 1.025 . The existence of critical Hartmann number is due to the fact that applying transverse magnetic field in a positive direction of the axis y and transverse electric field in the opposite direction of the axis z, respectively, creates a simultaneous applying of deterrent force and a driving force to the fluid in the microchannel. The effect of these two forces in the momentum equation is inserted as σE$_z$B$_y$ − σuB$_y^2$. In a constant transverse electric field, as long as by increasing the amount of magnetic field the total of two stated terms is a positive value, a force in line with the flow is applied to the fluid and increases the flow velocity. However, the process of increase in the flow velocity reduces as the magnetic field gradually increases. Then at a specific value of the magnetic field, corresponding to the critical Hartmann number (Ha$_{cr}$), the increase in velocity stops and from then by increasing the magnetic field, the volumetric force applied to the fluid is reduced. Fig. 6 has only covered two specific values of the transverse electric field; however, this process can be generalized to different transverse electric fields. For this purpose, for various values of the parameter of non-dimensional transverse electric field S in a similar way, Ha$_{cr}$ is calculated. Fig. 7 shows Ha$_{cr}$ in terms of S. Fig. 7 consists of two parts: the first part in which the critical Hartmann numbers has been shown in terms of the amount of transverse electric field S in the non-dimensional pressure difference Ω = 1. for S > 1 and the second part has been shown for values S ≤ 1. Chakraborty *et al.* (2013) by plotting Nusselt number in terms of Hartmann number in different transverse electric fields stated that in some of the transverse electric fields 0.8 ≤ S ≤ 100 , there are two distinct flow regimes. In the first regime, by increasing the Hartmann number, the value of Nusselt decreases and in the second regime by increasing the Hartmann number the value of Nusselt number increases. When the Hartmann number changes for this reason, they call it critical Hartmann number. It also stated that in the range of 0.8 ≤ S ≤ 100, Hartmann number is located within the range of 0.7 ≤ Ha$_{cr}$ ≤ 2 and for values of S < 0.8 critical Hartman number is no longer existed. However, the results of present work show that by increasing S, value of critical Hartmann number increases rapidly at first and then its growth rate slows. According to Fig. 7, it can be said critical Hartmann number for values of S > 100 tends toward a specified amount (about 1.5). Fig.8 has plotted the average velocity of the fluid in the microchannel in case of applying Hacr to the flow, according to different values of S for Ω = 1 and K=4. By using these figures, maximum rate and flow rate from the microchannel can be achieved for a certain amount of transverse electric field. In Fig. 9 critical Hartmann number in terms of non-dimensional transverse electric field S for α =

4500 , K=4 , has been plotted at various pressure differences. As can be seen, by increasing the axial pressure difference, the critical Hartmann number decreases. Because, by an increase in the pressure difference, the force caused by applying the external magnetic field to the fluid, decreases and the force caused by the pressure difference increases. If the pressure difference increases, the flow velocity in the microchannel increases. Therefore, the term of σuB$_y^2$, on the right hand side of the momentum equation in the direction of the axis x will have higher values and as a result, the total two right hand side terms of the momentum equation σE$_z$B$_y$ − σuB$_y^2$ reaches to its maximum at a lower Hartmann number. Fig. 10 has plotted critical Hartmann number in terms of non-dimensional pressure difference influenced by the non-dimensional axial electric field α = 4500 , K=4 and three different values for transverse electric field. As can be seen with an increase in the amounts of the transverse electric field, the decreasing trend in the critical Hartmann number becomes less due to the increase in pressure difference. Therefore, it can be said at the high values of transverse electric fields, the effect of pressure difference on the behavior of the critical Hartmann number becomes less.
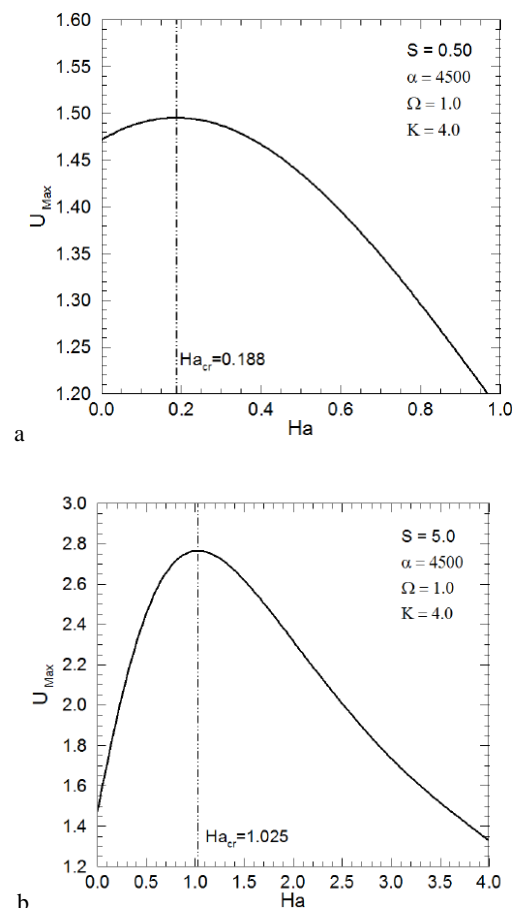

a

b

Fig. 6. Developed maximum velocity diagram of the flow in microchannel under the influence of α = 4500, K=4, Ω = 1 according to Hartmann number for a. S=0.5, b. S=5.
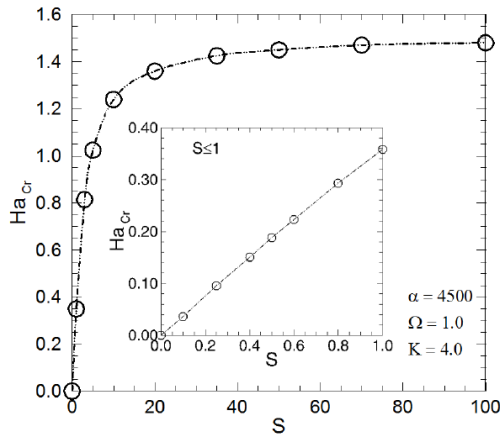
Fig. 7. Diagram of critical Hartmann numbers in terms of transverse electric field.
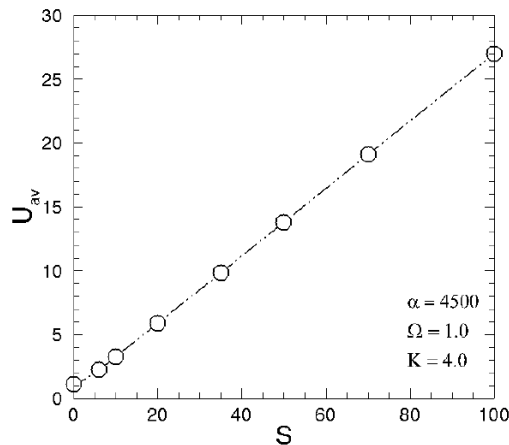

Fig. 8. Mean flow velocity diagram in terms of the transverse electric field in the critical Hartmann numbers.
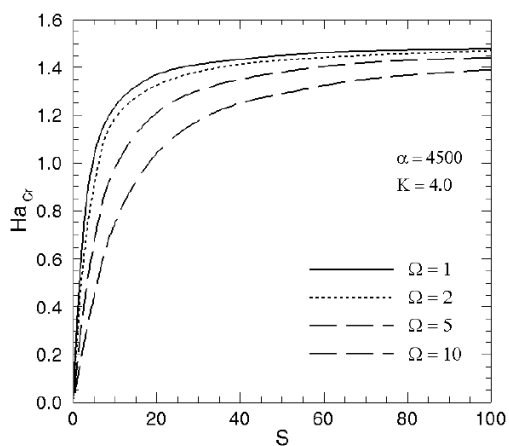

Fig. 9. Diagram of critical Hartmann numbers in terms of parameter S for different non-dimensional pressures.
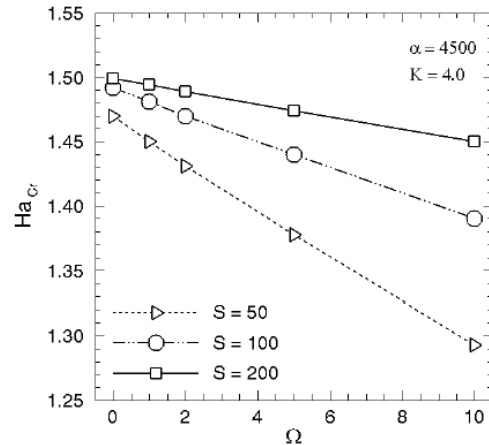

Fig. 10. Diagram of critical Hartmann number in terms of non-dimensional pressure for different values of the non-dimensional transverse electric field.

4. CONCLUSION

In the present work, electromagnetic hydrodynamic flow (EMHD) of electrolyte solution consisting of an axial electric field and traverse magnetic and electric fields inside the two-dimensional microchannel was studied. Flow equations were solved numerically by assuming non-slip condition on the walls and under a constant pressure gradient. By defining critical Hartmann number (Ha_{cr}) as the Hartmann number for which the maximum flow rate and consequently the maximum flow velocity is created, the critical Hartmann number for various values of the non-dimensional transverse electric field (S) is obtained. For this purpose, by plotting the diagram of maximum velocity as a function of Hartmann number in each non-dimensional transverse electric field, the Hartmann number for which the maximum velocity U_{max} is achieved has been selected as the critical Hartmann number. Therefore, the critical Hartmann numbers for different values of the transverse electric field were obtained in the range of $0 < S < 100$, and it became clear that with this criterion for all values of S, Hartmann number is critical. This result is in contrast with the result of Chakraborty *et al.* (2013) which has suggested that for values of $S < 0.8$, critical Hartman number no longer exists. The results showed that in the non-dimensional axial electric field $\alpha = 4500$ and non-dimensional Debye-Huckel parameter K = 4, By increasing the amount of S, Hacr number tends toward a constant value (about 1.5). It has also been shown that by increasing the amount of non-dimensional pressure difference, for each specific value of number S, the number Ha_{cr} is reduced. However, the effect of pressure changes on Ha_{cr} number in high values of number S reduces. Moreover, it can be said that in high values of S, the pressure differences on the critical Hartmann number are less effective.

REFERENCES

Al-Habahbeh, O., M. Al-Saqqa, M. Safi and T. A. Khater (2016). Review of magnetohydrodynamic pump applications. *Alexandria Engineering Journal* 55(2), 1347–1358.

Arulanandam, S. and D. Li (2000). Liquid transport in rectangular microchannels by electroosmotic pumping. *Colloids and Surfaces A: Physicochemical and Engineering Aspects* 161(1), 89–102.

Burgreen, D. and F. Nakache (1964). Electrokinetic flow in ultrafine capillary slits1. *The Journal of Physical Chemistry* 68(5), 1084–1091.

Chakraborty, R., R. Dey and S. Chakraborty (2013). Thermal characteristics of electromagnetohydrodynamic flows in narrow channels with viscous dissipation and joule heating under constant wall heat flux. *International Journal of Heat and Mass Transfer* 67, 1151–1162.

Chakraborty, S. and D. Paul (2006). Microchannel flow control through a combined electro-magnetohydrodynamic transport. *Journal of Physics D: Applied Physics* 39(24), 5364–5371.

Davidson, P. A. (2001). *An introduction to magnetohydrodynamics*, Volume 25. Cambridge university press.

Deng, S., Y. Jian, Y. Bi, L. Chang, H. Wang and Q. Liu (2012). Unsteady electroosmotic flow of power-law fluid in a rectangular microchannel. *Mechanics Research Communications* 39(1), 9–14.

Escandón, J., F. Santiago, O. Bautista and F. Méndez (2014). Hydrodynamics and thermal analysis of a mixed electromagnetohydrodynamic-pressure driven flow for phanthien–tanner fluids in a microchannel. *International Journal of Thermal Sciences* 86, 246–257.

Hunter, R. J. (2013). *Zeta potential in colloid science: principles and applications*, Volume 2. Academic press.

Jang, J. and S. S. Lee (2000). Theoretical and experimental study of mhd (magnetohydrodynamic) micropump. *Sensors and Actuators A: Physical* 80(1), 84–89.

Karniadakis, G. E., A. Beskok and N. Aluru (2006). *Microflows and nanoflows: fundamentals and simulation*, Volume 29. Springer Science & Business Media.

Kiyasatfar, M. and N. Pourmahmoud (2016). Laminar mhd flow and heat transfer of power-law fluids in square microchannels. *International Journal of Thermal Sciences* 99, 26–35.

Lahjomri, J., K. Zniber, A. Oubarra and A. Alemany (2003). Heat transfer by laminar hartmann's flow in thermal entrance region with uniform wall heat flux: the graetz problem extended. *Energy conversion and Management* 44(1), 11–34.

Levine, S., J. Marriott, G. Neale and N. Epstein (1975). Theory of electrokinetic flow in fine cylindrical capillaries at high zeta-potentials. *Journal of Colloid and Interface Science* 52(1), 136–149.

Li, D. (2004). *Electrokinetics in microfluidics*, Volume 2. Academic Press.

Li, D. (2008). Encyclopedia of microfluidics and nanofluidics. *Springer Science & Business Media.*

Masliyah, J. H. and S. Bhattacharjee (2006). *Electrokinetic and colloid transport phenomena.* John Wiley & Sons.

Nguyen, N. T. and S. T. Wereley (2002). *Fundamentals and applications of microfluidics.* Artech House.

Patankar, N. A. and H. H. Hu (1998). Numerical simulation of electroosmotic flow. *Analytical Chemistry* 70(9), 1870–1881.

Reuss, F. F. (1809). Sur un nouvel effet de l''electricite' galvanique. Mem. Soc. Imp. Natur. Moscou 2, 327–337.

Rice, C. and R. Whitehead (1965). Electrokinetic flow in a narrow cylindrical capillary. *The Journal of Physical Chemistry* 69(11), 4017–4024.

Wang, L., Y. Jian, Q. Liu, F. Li and L. Chang (2016). Electromagnetohydrodynamic flow and heat transfer of third grade fluids be-tween two micro-parallel plates. *Colloids and Surfaces A: Physicochemical and Engineering Aspects* 494, 87–94.

Wang, P. J., C. Y. Chang and M. L. Chang (2004). Simulation of two-dimensional fully developed laminar flow for a magneto-hydrodynamic (mhd) pump. *Biosensors and Bioelectronics* 20(1), 115–121.

Yang, C. and D. Li (1997). Electrokinetic effects on pressure-driven liquid flows in rectangular microchannels. *Journal of colloid and interface science* 194(1), 95–107.